The Effect of Hydrogen Peroxide on the Synthesis of Terephthalate-Based Metal-Organic Frameworks

Rebeca Monteagudo-Olivan,[a] Isabel Jiménez-Fernández,[a] Pilar López-Ram-de-Viu,[b] Victor Sebastian,*[a,c] and Joaquín Coronas*[a]

Abstract: MOFs (metal-organic frameworks) are versatile materials for a number of applications dealing with environment, energy and health topics. A novel synthesis route is presented in this work with the objective of enhancing the production of MOFs. This is triggered by hydrogen peroxide (H_2O_2) to promote the synthesis of terephthalate-based MOFs of MIL-53 and MIL-68 types, specifically those made from Fe^{3+} and Al^{3+} and mixtures of both. The different characterization techniques (TGA, XRD, SEM, TEM, N_2 porosimetry and Raman, mass and NMR spectroscopies) allowed to gain insight into the H_2O_2 effect on the MOF synthesis. Reaction yield was significantly improved (the highest yield being 74% for MIL-53(Al)), while crystallinity and N_2 adsorption properties were mostly maintained for phases based on Al and Al/Fe. Furthermore, a reaction mechanism was envisaged from the mass spectroscopy analysis of the synthesis solutions, suggesting for H_2O_2 a role of μ-hydroxo bridge promoter, favoring the link between terephthalate ligands and aluminum containing species to give rise to the μ-carboxylate bridges, leading to a faster growth of the final MOF, and offering a novel MOF synthesis approach.

The efficient synthesis of MOFs is a decisive point for the industrial use of these materials, which are effective in several key applications related to gas separations and storage,[1] selective membranes,[2] catalysis,[3] encapsulation[4,5] and medicine,[6] among others. The commonest synthesis method is the solvo- or hydrothermal, in which the precursors, i.e. a metal salt and an organic ligand, are dispersed in an organic solvent or water.[7,8] The mixture can be heated up at high temperature (working under autogenous pressure) for relatively long reaction times.

Several methodologies are reported as alternative to the classic solvothermal synthesis. The most studied are the microwave[9] and the sonochemical[10] assisted syntheses, which require a more complicated setup. These methods increase nucleation through the perturbances that they create in the media. Consequently, they affect crystallization and growth, differently to the basic solvothermal method.[8] Other remarkable methods, the mechanosynthesis and high pressure driven synthesis, i.e. in absence of solvents, have been proved useful, but only with a few MOFs.[8,11]

Alternatively to external physical modifications, *in situ* chemical variations have been successfully described, such as the coordination modulation approach,[12,13] the use of some additives[14–16] and the application of reactive gas atmospheres.[17] In liquid phase, to modulate the synthesis, a monodentante ligand is added to the media, such as monocarboxylate or amine ligand, that typically improves the crystallinity of the MOF and can modify its shape.[12,13,18] Other chemicals can influence the size, shape or surface of MOF particles, such as surfactants[14,15] and blocking agents.[16] Regarding the modification of the reaction atmospheres, CO or O_2 at high pressure have been used to improve the crystallinity and to accelerate the synthesis, allowing the creation of bimetallic MOF particles with different profiles of metal composition.[17]

Hydrogen peroxide (H_2O_2) is a common reactant and a strong oxidant used in a wide variety of applications such as water treatment, pulp and textile bleaching, and chemical synthesis, among others.[19] In water and soil treatment, it is well-known the Fenton reactions to boost hydroxyl radical formation thanks to the reaction of H_2O_2 with iron ions[20,21] to remove persistent organic pollutants, promoting their oxidation.[19] Representative Fenton reactions are as follows:

$H_2O_2 + Fe^{2+} \rightarrow {}^{\cdot}OH + Fe^{3+} + OH^-$ (1)

$H_2O_2 + Fe^{3+} \rightarrow HO_2^{\cdot} + Fe^{2+} + H^+$ (2)

with respective k values of 51 $M^{-1}s^{-1}$ and 0.01 $M^{-1}s^{-1}$, in aqueous media at room temperature.[22] Equation (2) is disfavored compared to (1), although (2) is favored in high concentrated solutions of Fe^{3+}.[23] In bleaching, hydrogen peroxide removes the organic components. In chemical synthesis, H_2O_2 role can turn complex. For example, it can promote, in presence of Fe^{2+}, the hydroxylation of tartaric acid[20] and terephthalic acid,[24] or the epoxidation of alkenes.[25,26]

Considering previous results reported by our group in which the crystallization of MOFs was accelerated in oxidant gas atmospheres,[17] it was hypothesized the use of H_2O_2 as a MOF synthesis promoter. Specifically, it has been proven effective on the synthesis of terephthalate-based MOFs with trivalent metals (Fe^{3+} and Al^{3+}), which, to the best of our knowledge, has not been previously described in the synthesis of hybrid microporous materials. Firstly, we performed reference experiments to observe the effect of stablished conditions on the final obtained MOF (see Figs. 1 and S1 and S2, Tables 1 and S1), considering that the basis conditions studied here are not the same as those reported.[27–30] The addition of H_2O_2 (x1 and x2 equivalents or molar proportion with respect to the reactants)

[a] Dr. R. Monteagudo, I. Jiménez, Dr. V. Sebastian and Prof. J. Coronas
Chemical and Environmental Engineering Department, Instituto de Nanociencia de Aragón (INA) and Instituto de Materiales de Aragón (ICMA), Universidad de Zaragoza-CSIC, 50018 Zaragoza, Spain.
E-mail: victorse@unizar.es, coronas@unizar.es
[b] Dr. P. López-Ram-de-Viu
Departamento de Química Orgánica, Universidad de Zaragoza, and Instituto de Síntesis Química y Catálisis Homogénea (Universidad de Zaragoza-CSIC), 50009 Zaragoza, Spain.
[c] Dr. V. Sebastian
Networking Research Center on Bioengineering, Biomaterials and Nanomedicine, CIBER-BBN, 28029 Madrid, Spain

Supporting information for this article is given via a link at the end of the document

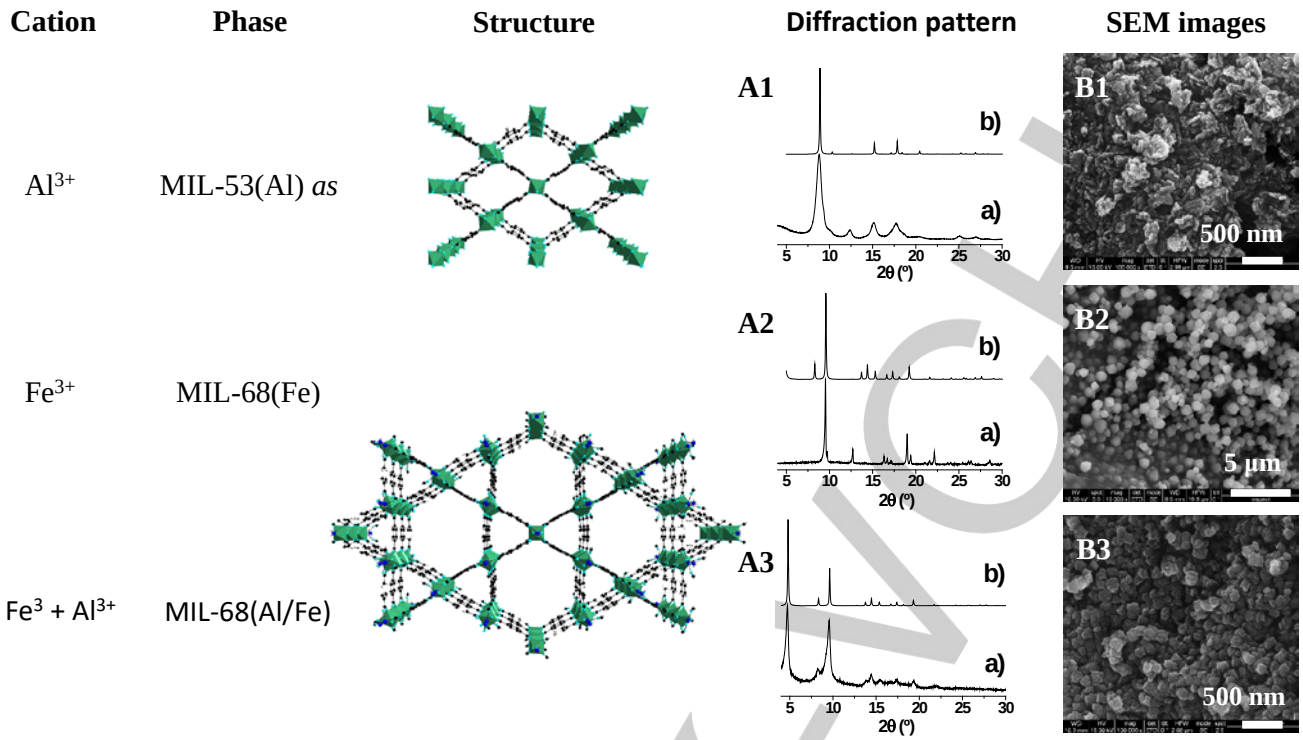

Figure 1. Final phases obtained with Fe^{3+}, Al^{3+} or an equimolar blend of both for 1.25 h, their respective diffraction patterns (A1a, A2a and A3a) compared with the simulated (A1b, A2b and A3b, CIFs 220475, 778931 and 222072), [27,28,31,32] and the SEM images of each phase (B1-B3). No H_2O_2 was used in these runs

Table 1. Reaction conditions for the three sets of experiments at 90 ºC. Molar ratios of metal ions, terephthalic acid and solvent for all runs were $2M^{3+}$ (M=Al^{3+}, Fe^{3+} or Al^{3+}/ Fe^{3+}, equimolar):$2H_2BDC$:129DMF, without H_2O_2, and with H_2O_2 at molar proportions 1 and 2 (x1 and x2).

M(s)	Molar ratio	Run (0x H_2O_2)	Run (x1 H_2O_2)	Run (x2 H_2O_2)	Time
Al	2Al:2H_2BDC	1.1	2.1	3.1	1.25 h
		1.2	2.2	3.2	2.25 h
Fe	2Fe:2H_2BDC	1.3	2.3	3.3	1.25 h
		1.4	2.4	3.4	2.25 h
Al/Fe	1Al:1Fe:2H_2BDC	1.5	2.5	3.5	1.25 h
		1.6	2.6	3.6	2.25 h

to the synthesis media of MIL-53(Al) produced an important increment of the reaction yield (Table 2), being more remarkable for 1.25 h, when the yield increased from 5% to 49% (runs **1.1**, **2.1** and **3.1**). The highest yield of 74% (Table 2) was obtained for 2.25 h and a H_2O_2 molar ratio x2 (run **3.2**). As shown in Fig. S3, the XRD intensities corresponding to the samples obtained in presence of H_2O_2 appear at the same 2·theta values than in both the simulated and the blank experiments (no H_2O_2) patterns. Besides, the peaks in the diffraction patterns appeared wider in the runs with increasing amount of H_2O_2, suggesting a loss of crystallinity or changes in crystal size. However, BET areas remained similar for all experiments (the highest value of 1245 m^2/g obtained in run **2.2** with a H_2O_2 molar ratio x1), and close to the reported values for MIL-53(Al) (1140 m^2/g).[27] Particle size was maintained ca. 100 nm (see SEM and TEM images in Figs. S4 and S5). The BET specific surface area values and the XRD patterns suggest that in case of MIL-53(Al) a H_2O_2 molar ratio x1 was the optimum.

Regarding the MIL-53(Al) XRD patterns, Fig. S3 shows that the main peak at 8.7º shows a shoulder at 9.3º, and a peak at 12.5º also appeared with low intensity for some samples (runs **1.1** and **3.1** and **3.2**, with no H_2O_2 and the largest amount of it, respectively). This is in agreement with the presence of a part of the material in the hydrated form, as can be inferred from the comparison with the simulated pattern of the hydrated or *lt* form, in which water molecules are bound by hydrogen bonds to adjacent carboxylates of terephthalate that narrow the pores and give rise to different diffraction patterns.[27] Raman spectroscopy highlights these different configurations (Fig. S6 and Table S2). Significant shifts of the carboxylate bands were observed, as hydrogen bonds are lacking, compared to the Raman spectrum of MIL-53 *lt*, while the vibrations corresponding to aromatic stretching and deformations are mainly kept. The band at 179 cm^{-1} of MIL-53(Al) synthesized here is also a remarkable difference, the network in the open pore form shows a lattice vibration (contraction and expansion) of the network (as it is displayed for carbon nanotubes in the radial breathing mode).[33]

Table 2. Yield and BET area values for synthesis of MIL-53(Al), MIL-68(Fe) and MIL-68(Al/Fe) in different conditions (see Table 1).

	x0 H_2O_2			x1 H_2O_2			x2 H_2O_2		
t(h)	Run	%	BET area (m^2/g)	Run	%	BET area (m^2/g)	Run	%	BET area (m^2/g)
MIL-53(Al)									
1.25	1.1	5.0	-	2.1	27	824	3.1	49	1072
2.25	1.2	39	1145	2.2	40	1245	3.2	74	1025
MIL-68(Fe)									
1.25	1.3	4.1	-	2.3	0.5	-	3.3	18	-
2.25	1.4	6.2	186	2.4	4.7	-	3.4	36	53
MIL-68(Al/Fe)									
1.25	1.5	18	1189	2.5	31	1077	3.5	39	396
2.25	1.6	30	1235	2.6	48	1139	3.6	56	947

In addition, since the solid ^{13}C-NMR spectra were almost identical for common MIL-53(Al) and that obtained in presence of H_2O_2, the chemical environments of the carbon atoms (three different types of C atoms corresponding to the three main peaks in Fig. S7) showed no differences, even though the pore configuration was different for each sample.

All in all, for MIL-53(Al) syntheses a clear increase in yield was observed, as well as a preservation of textural properties and generation of similar particles (TEM images Fig. S54) with broadening diffraction peaks. H_2O_2 exhibited a clear promoter role on the synthesis, affecting the crystallization dynamics. Firstly, to explain the mechanism behind, the chemical modification of the ligand by hydroxylation (given the oxidant function of H_2O_2) of the aromatic ring of the terephthalic acid to form 2-hydroxyterephthalic acid was discarded from the Raman spectra. The shifts for the final phase of MIL-53(Al) treated with H_2O_2 showed the same band pattern of para-substituted aromatic ring, as the reference MIL-53(Al) obtained without H_2O_2 (Fig. S6 and Table S2).

Moreover, the reaction was studied by liquid ^{1}H- and ^{13}C-NMR, with and without H_2O_2, in order to understand why MIL-53(Al) formation evolves differently in presence of hydrogen peroxide. For these studies, an aliquot was taken after 45 min of reaction in both cases. For ^{1}H-NMR analysis, 0.5 mL of the studied solution was mixed with some drops of $CDCl_3$. Even if DMF (reaction solvent) and partially deuterated DMF (formed in the analysis mixture) signals were large, potential modifications could be observed in the linker terephthalic signals from the aromatic area. However, in agreement with the above mentioned Raman study (Fig. S6), the observed NMR peaks in the reactions with and without H_2O_2 were the same and they correspond to the terephthalic acid reference (Fig. S8).

The reaction was also analyzed by high resolution mass spectroscopy (HRMS), again with and without H_2O_2 (Fig. S9), to study if H_2O_2 modified the precursor chain of MIL-53(Al). One microliter of each sample, taken also at 45 min, was diluted in methanol and ionized using the positive electrospray ionization mode (ESI+). Without H_2O_2, several peaks at different *m*/*z* ratios were observed. The resolved peaks correspond to positive molecular ions in which Al^{3+} cations are linked by terephthalate bridges, and some molecules of the ionized solvent complete the coordination sphere of metal atoms (*m*/*z* 433 and 611) (Fig. 2a). A single unit was also observed, with one terephthalate ligand linked to the Al^{3+} nucleus (*m*/*z* 296) (Fig. 2b). In the sample with H_2O_2, the only observed peak corresponds to a single cation with two terephthalate ligands linked to one Al^{3+} nucleus (*m*/*z* 430) (Fig. 2c). In this sample, molecular ions with Al-µ-terephthalate-Al chains of Fig. 2b were not observed. Taking into account that a 1D structure is known to be present as a ribbon of aluminum linked through µ-OH and µ-terephthalate bridges,[27] it is plausible to suppose that µ-OH bridges were unstable to ionization conditions and they could not be detected, even if they were present, in the studied solutions.

A different mechanism of MOF nucleation is hypothesized to explain the differences between the observed species in HRMS with and without H_2O_2. Without H_2O_2, chains of terephthalate bridges would form first and be observable in HRMS. From these chains, µ-hydroxo bridges generate slowly to yield the MOF later. In presence of H_2O_2, µ-hydroxo bridges would form directly at first. Then, terephthalate links an aluminum nucleus (this molecular entity was observed through HRMS, obviously without OH bridges) (Fig. 2c), and finally µ-carboxylate bridges form easily between aluminum atoms that were already close. This difference in the mechanism of formation of µ-hydroxo bridges is consistent with a faster nucleation and growth and a higher reaction yield in presence of H_2O_2.

Regarding the role of DMF, in general, its use has been discussed not only as common solvent but sometimes as an *a priori* irreplaceable solvent in the MOF synthesis. Here, it completes the coordination around metal ions. The polar properties of DMF to dissolve the metal-ligand complexes and the acid pH, which allows to have the free cations in solutions, promote the precursor formation instead of inorganic polymerization or oxides formation.[34]

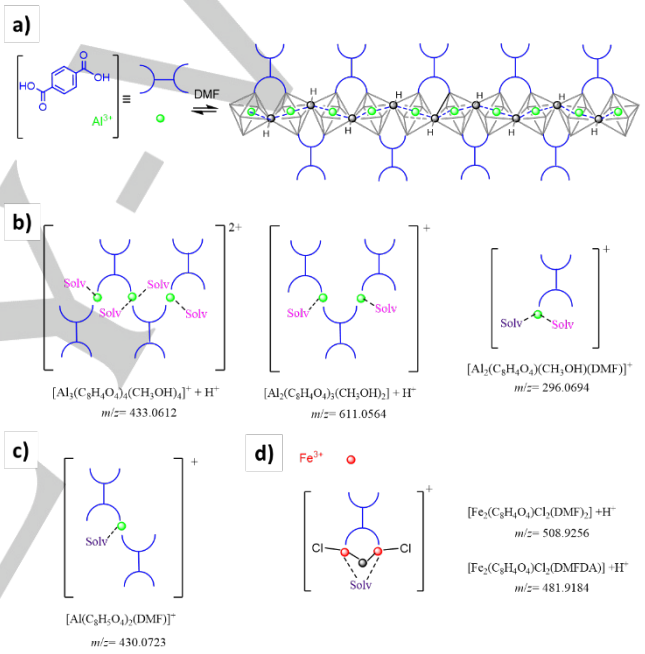

Figure 2. Chain precursor formation of µ-hydroxo and µ-terephthalate bridges to form MIL-53(Al) (a). MS fragments from MIL-53(Al) precursor syntheses without H_2O_2 (b) and with H_2O_2 (c). MS fragments from MIL-68(Fe) precursor synthesis (d). Color code: Al (green), Fe (red), bridge O (grey).

The approach followed with MIL-53(Al) was extended to Fe and Al/Fe terephthalates (with respective highest yield increases from 6.2% to 36% and from 30% to 56%) in order to explore the versatility of this novel synthesis method based on the use of H_2O_2. First, a solution of both metal salts in DMF (without H_2BDC) was treated in the same reaction system at the same conditions (90 ºC and 1.25 h) with and without H_2O_2. An orange solution was obtained without H_2O_2 (Fig. 3Aa). In presence of H_2O_2, the solution changed color (Fig. 3Ab, x1), with an increase of redness as the concentration of H_2O_2 was increased (Fig. 3Ab, x2), suggesting the formation of nanoparticles. The particles of the salt solution treated with x2 H_2O_2 (Fig. 3Ac) were recovered by centrifugation after 30 min of reaction and analyzed by TEM and STEM. Sharpened needle-shape nanoparticles (3-45 nm

wide and 100-550 nm length, depending on the agglomeration) were observed (Figs. 3B and 3C). The EDS analysis showed that the composition was based on iron (Fig. 3D), and no aluminum was detected at this reaction time. The formation of these particles could be explained from a redox process. As mentioned in the introduction, the combination of Fe^{3+} and H_2O_2 is well-known for producing Fenton reactions. The generation of $HO_2^{\cdot}$ species and Fe^{2+} is possible due to the great excess Fe^{3+} used, and maybe favored by the relatively high temperature. This could lead to the formation of particles of mixed valence iron complexes. Nevertheless, Fenton reactions produce hydroxyl radicals ·OH that might lead to the quick transformation of terephthalic acid into 2-hydroxyterephthalic acid, but this fact was discarded from Raman spectra as discussed above. Moreover, neither the solution reactions (Fig. 3A) nor the obtained MOFs with Fe^{3+} (with or without H_2O_2) showed fluorescence with a UV lamp at 254 or 365 nm corresponding to 2-hydroxyterephthalic acid.[24] Otherwise, and from an oxidation point of view, H_2O_2 could have promoted the formation of iron oxides that condense at the working conditions, these species being responsible for the color change observed in the reactions with hydrogen peroxide. This oxide was expected to be formed in higher extension for the sole iron synthesis, and Raman bands at 332 and 447 cm^{-1} (Fig. S6 and Table S2) attributed to Fe-O bond vibrations of oxides and hydroxides seem to corroborate it, as they are not observed in the other phases.

A yield increase was observed for both syntheses, MIL-68(Fe) and MIL-68(Al/Fe) (Table 2). However, the yield only raised its value by using the double proportion of H_2O_2 in case of MIL-68(Fe) (**3.3** and **3.4**). In fact, it decreased significantly for 1.25 h and x1 H_2O_2 (**2.3**). The formation of the described sharp particles with H_2O_2, using just the metal salts and the solvent, could hinder the MOF growth first.

The study by HRMS of the reaction with H_2O_2 revealed the existence of iron dimers with both μ-oxo and μ-terephthalic bridges between both iron nuclei. One chloride atom (coming from the ferric chloride used as reactive) linked to each metal atom and with some small molecules (DMF or N,N-dimethylformamide dimethylacetal, DMFDA, formed by reaction of DMF with methanol upon ionization) complete the coordination sphere of metal atoms (Figs. 2d and S10). Hydrogen peroxide could increase the formation of oxygen bridges between Fe^{3+}, as described above for aluminum, or increase the formation of ferric oxides.

Regarding the textural properties, the BET specific surface areas were low for all MIL-68(Fe) samples (see Table 2) and some experiments did not yield enough amount of powder for the measurements. Moreover, the reported experimental value for MIL-68(Fe) is relatively low, 355 m^2/g, with a previous degasification at 250 ºC.[28] A temperature of 200 ºC was used here, which may justify the lower values obtained. The BET areas in the mixed phase MIL-68(Al/Fe) were slightly reduced, particularly with x2 H_2O_2. This can be explained by the increase of the iron content when more H_2O_2 was added, comparing the respective values in the pure phases (low for Fe-based and high for Al-based MOFs) and the color change observed for the final phases (Fig. 3E). For example, in the 2.25 h experiments, the BET area values were with x2 H_2O_2 1025 m^2/g for MIL-53(Al) (**3.2**), 53 m^2/g for MIL-68(Fe) (**3.4**) and 947 m^2/g for mixed MIL-68(Al/Fe) (**3.6**, orange color), meanwhile for those without H_2O_2, 1145 m^2/g for MIL-53(Al) (**1.2**), 186 m^2/g for MIL-68(Fe) (**1.4**) and 1235 m^2/g for mixed MIL-68(Al/Fe) (**1.6**, raw white color). Besides that, a differentiated low value was obtained at 1.25 h and x2 H_2O_2 for MIL-68(Al/Fe) (**3.5**), 396 m^2/g, in agreement with the lower crystallinity (Fig. S11). MIL-68(Al) can exhibit a BET area as high as ca. 1400 m^2/g,[31] what agrees with the fact that the highest BET area sample (**1.6**) was almost white consistent with a low or null Fe content.

For MIL-68(Al/Fe), no significant changes were observed in crystallinity (Fig. S10) or in morphology in SEM images (Fig. S12) comparing the reference samples with those produced in H_2O_2, except for the diffraction pattern of sample synthesized for 1.25 h with x2 H_2O_2 (**3.5**) in agreement with the low BET area.

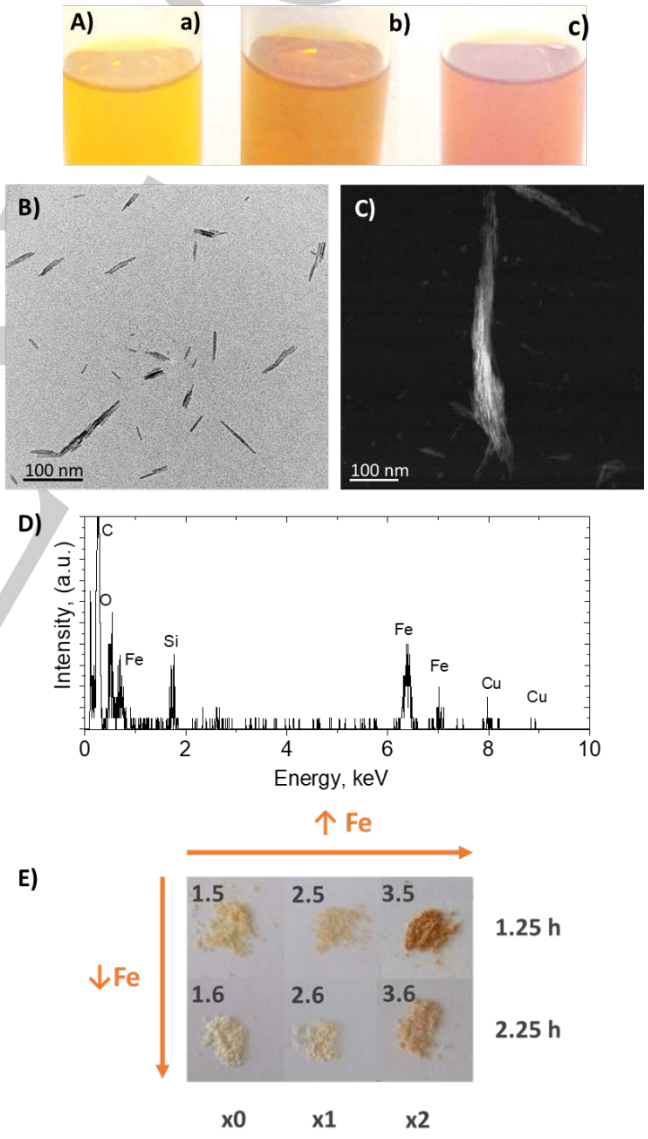

Figure 3. Photos corresponding to the solutions of Fe^{3+} and Al^{3+} metal salts after 1.25 h (A) of blank (a), x1 H_2O_2 (b) and x2 H_2O_2 (c); TEM (B) and STEM-HAADF (C) images of the particles recovered from A(c); and EDS analysis profile (D) of (C). Photos of the obtained solids in the Al^{3+}/Fe^{3+}-terephthalate experiments (E).

This diffraction pattern might be compatible with that corresponding to a mixture of MIL-53(Al) and MIL-53(Fe), the latter not presenting an appreciable BET area.[35] Additionally, considering the excess of promoter (x2 H_2O_2) and the reduced time, more nuclei were formed and the growth of particles (Fig. 3A) was limited by the shorter time. In case of MIL-68(Fe), the morphology was noticeably modified, the reference rhombohedral particles turned into polydisperse rods for samples with x2 H_2O_2 (Fig. S13). In fact, it was observed an increased XRD background and peak broadening, therefore some crystallinity was lost (Fig. S14).

Summarizing, H_2O_2 produced an increase of synthesis yield for MIL-53(Al) and MIL-68(Al/Fe), while MIL-68(Fe) seemed to be impure by the presence of some oxide. The crystallinity and the BET area were roughly kept for MIL-53(Al) and MIL-68(Al/Fe). For iron-based phases, the formation of needle-like particles of iron oxide was favored with H_2O_2, and mixed MOFs with different iron content were produced by controlling the synthesis time and the amount of H_2O_2. In case of Al containing MOFs, the hydrogen peroxide would promote the early formation of μ-hydroxo bridges and then terephthalate ligands would link aluminum containing species to give rise to the μ-carboxylate bridges between metallic atoms already close, leading to a faster growth of the final MOF. Contrarily, in absence of H_2O_2 chains of terephthalate bridges would form first, delaying the synthesis of the MOF. Finally, regarding the amount of H_2O_2 used, a H_2O_2 molar ratio x1 seemed to the the optimum from the point of view of both the BET specific surface area values and the appearednce of the XRD patterns more close to the simulated.

Acknowledgements

The authors thank financial support from the Spanish MINECO and FEDER (MAT2016-77290-R), Aragón Government (T43-17R & E102) and the People Program (CIG-Marie Curie Actions, REA grant agreement no. 321642). CIBER-BBN is an initiative funded by the VI National R&D&i Plan 2008–2011 financed by the Instituto de Salud Carlos III with the assistance of the European Regional Development Fund.

Keywords: aluminium • bridging ligands • iron • metal-organic frameworks• hydrogen peroxide

[1] R. J. Kuppler, D. J. Timmons, Q.-R. Fang, J.-R. Li, T. A. Makal, M. D. Young, D. Yuan, D. Zhao, W. Zhuang, H.-C. Zhou, *Coord. Chem. Rev.* **2009**, *253*, 3042–3066.

[2] S. Sorribas, P. Gorgojo, C. Téllez, J. Coronas, A. G. Livingston, *J. Am. Chem. Soc.* **2013**, *135*, 15201–15208.

[3] J. Lee, O. K. Farha, J. Roberts, K. A. Scheidt, S. T. Nguyen, J. T. Hupp, *Chem. Soc. Rev.* **2009**, *38*, 1450.

[4] L. Paseta, G. Potier, S. Abbott, J. Coronas, *Org. Biomol. Chem.* **2015**, *13*, 1724–1731.

[5] R. Monteagudo-Olivan, L. Paseta, G. Potier, P. López-Ram-de-Viu, J. Coronas, *Eur. J. Inorg. Chem.* **2019**, 29–36.

[6] P. Horcajada, T. Chalati, C. Serre, B. Gillet, C. Sebrie, T. Baati, J. F. Eubank, D. Heurtaux, P. Clayette, C. Kreuz, J. S. Chang, Y. K, Hwang, V. Marsaud, P. N. Bories, L. Cynober, S. Gil, G. Férey, P. Couvreur, R. Gref, *Nat Mater* **2010**, *9*, 172–178.

[7] O. K. Farha, J. T. Hupp, *Acc. Chem. Res.* **2010**, *43*, 1166–1175.

[8] N. Stock, S. Biswas, *Chem. Rev.* **2012**, *112*, 933–969.

[9] J. Klinowski, F. A. A. Paz, P. Silva, J. Rocha, *Dalton Trans.* **2011**, *40*, 321–330.

[10] N. A. Khan, S. H. Jhung, *Coord. Chem. Rev.* **2015**, 285, 11–23.

[11] L. Paseta, G. Potier, S. Sorribas, J. Coronas, *ACS Sustain. Chem. Eng.* **2016**, *4*, 3780–3785.

[12] T. Tsuruoka, S. Furukawa, Y. Takashima, K. Yoshida, S. Isoda, S. Kitagawa, *Angew. Chemie - Int. Ed.* **2009**, *48*, 4739–4743.

[13] S. Diring, S. Furukawa, Y. Takashima, T. Tsuruoka, S. Kitagawa, *Chem. Mater.* **2010**, *22*, 4531–4538.

[14] W. W. Xiong, Q. Zhang, *Angew. Chemie - Int. Ed.* **2015**, *54*, 11616–11623.

[15] B. Seoane, A. Dikhtiarenko, A. Mayoral, C. Tellez, J. Coronas, F. Kapteijn, J. Gascon, *CrystEngComm* **2015**, *17*, 1693–1700.

[16] N. Stock, S. Biswas, *Chem. Rev.* **2012**, *112*, 933–969.

[17] R. Monteagudo-Olivan, M. Arruebo, P. López-Ram-De-Viu, V. Sebastian, J. Coronas, *J. Mater. Chem. A* **2018**, *6*, 14352–14358.

[18] A. Umemura, S. Diring, S. Furukawa, H. Uehara, T. Tsuruoka, S. Kitagawa, *J. Am. Chem. Soc.* **2011**, *133*, 15506–15513.

[19] E. Brillas, I. Sirés, M. A. Oturan, *Chem. Rev.* **2009**, *109*, 6570–6631.

[20] H. J. H. Fenton, *J. Chem. Soc. Trans.* **1894**, *65*, 1894.

[21] F. Haber, J. Weiss, *Proc. R. Soc. A Math. Phys. Eng. Sci.* **1934**, *147*, 332–351.

[22] E. Petrucci, A. Da Pozzo, L. Di Palma, *Chem. Eng. J.* **2016**, *283*, 750–758.

[23] M. Hayyan, M. A. Hashim, I. M. Alnashef, *Chem. Rev.* **2016**, *116*, 3029–3085.

[24] J. C. Barreto, G. S. Smith, N. H. P. Strobel, P. A. McQuillin, T. A. Miller, *Life Sci.* **1994**, *56*, PL89–PL96.

[25] B. S. Lane, K. Burgess, *Chem. Rev.* **2003**, *103*, 2457–2474.

[26] G. Grigoropoulou, J. H. Clark, J. A. Elings, *Green Chem.* **2003**, *5*, 1–7.

[27] T. Loiseau, C. Serre, C. Huguenard, G. Fink, F. Taulelle, M. Henry, T. Bataille, G. Férey, *Chemistry* **2004**, *10*, 1373–1382.

[28] A. Fateeva, P. Horcajada, T. Devic, C. Serre, J. Marrot, J.-M. Grenèche, M. Morcrette, J.-M. Tarascon, G. Maurin, G. Férey, *Eur. J. Inorg. Chem.* **2010**, 3789–3794.

[29] Q. Yang, S. Vaesen, M. Vishnuvarthan, F. Ragon, C. Serre, A. Vimont, M. Daturi, G. De Weireld, G. Maurin, *J. Mater. Chem.* **2012**, *22*, 10210.

[30] M. Schubert, U. Mueller, S. Marx, *WO Pat., 2008/12905, Aktiengesellschaft, BASF*, **2008**, 12905.

[31] B. Seoane, V. Sebastián, C. Téllez, J. Coronas, *CrystEngComm* **2013**, *15*, 9483–9490.

[32] K. Barthelet, J. Marrot, G. Ferey, D. Riou, *Chem. Commun. (Camb).* **2004**, 520–521.

[33] J. Maultzsch, H. Telg, S. Reich, C. Thomsen, *Phys. Rev. B - Condens. Matter Mater. Phys.* **2005**, *72*, 205438.

[34] T. Devic, C. Serre, *Chem. Soc. Rev.* **2014**, *43*, 6097–6115.

[35] M. S. Denny, S. M. Cohen, *Angew. Chemie - Int. Ed.* **2015**, *54*, 9029–9032.

Entry for the Table of Contents

COMMUNICATION

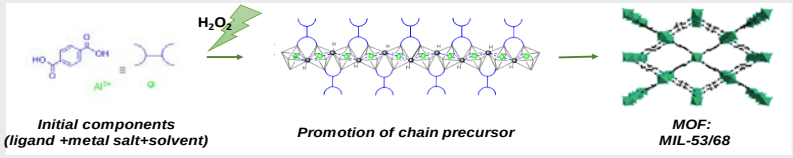

A synthesis route is presented with the objective of enhancing the production of MOFs. This is triggered by H_2O_2 to promote the synthesis of terephthalate-based MOFs of MIL-53 and MIL-68 types, specifically those made from Fe^{3+} and Al^{3+} and mixtures of both. A reaction mechanism was envisaged suggesting for H_2O_2 a role of μ-hydroxo bridge promoter, favoring the link between terephthalate ligands and aluminum containing species to give rise to the μ-carboxylate bridges, leading to a

Rebeca Monteagudo-Olivan, Isabel Jiménez-Fernández, Pilar López-Ram-de-Viu, Víctor Sebastián, and Joaquín Coronas**

Page No. – Page No.

The Effect of Hydrogen Peroxide on the Synthesis of Terephthalate-Based Metal-Organic Frameworks

[a] Dr. R. Monteagudo, I. Jiménez, Dr V. Sebastian and Prof. J. Coronas
Chemical and Environmental Engineering Department, Instituto de Nanociencia de Aragón (INA) and Instituto de Materiales de Aragón (ICMA), Universidad de Zaragoza-CSIC, 50018 Zaragoza, Spain.
E-mail: victorse@unizar.es, coronas@unizar.es
[b] Dr. P. López-Ram-de-Viu
Departamento de Química Orgánica, Universidad de Zaragoza, and Instituto de Síntesis Química y Catálisis Homogénea (Universidad de Zaragoza-CSIC), 50009 Zaragoza, Spain
[c] Dr V. Sebastian
Networking Research Center on Bioengineering, Biomaterials and Nanomedicine, CIBER-BBN, 28029 Madrid, Spain